Online Supplemental Material for

Kenter et al. http://www.jem.org/cgi/doi/10.1084/jem.20031935

Information for Figure S1. Microhomology between the Sμ and the downstream S regions is a common feature in switch junctions. In pG3.1 and pG3.02s, the range of overlap between Sμ and Sγ3 was normal (1–10 bps), but the average length of overlap was longer than in endogenous Sμ/Sγ3 junctions, perhaps as a result of their extrachromosomal context. At endogenous loci derived from LPS-activated B cells, mutations accumulate around switch junctions (Dunnick, W., M. Wilson, and J. Stavnezer. 1989. *Mol. Cell. Biol.* 9:1850–1856; Dunnick, W., G.Z. Hertz, L. Scappino, and C. Gritzmacher. 1993. *Nucleic Acids Res.* 21:365–372; Dunnick, W., and J. Stavnezer. 1990. *Mol. Cell. Biol.* 10:397–400). Mutations at S/S junctions were also observed in recombinant switch substrates (unpublished data).

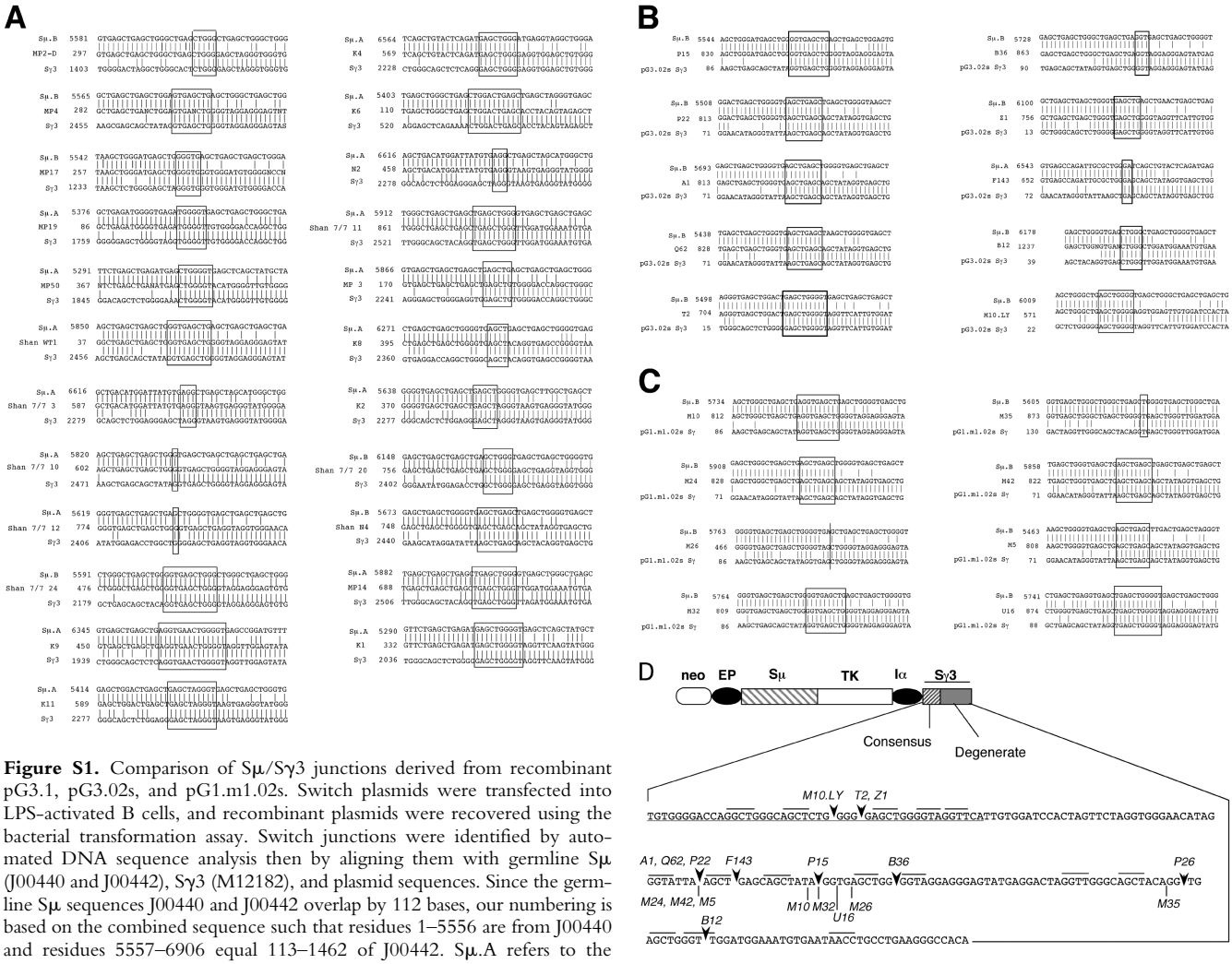

Figure S1. Comparison of Sμ/Sγ3 junctions derived from recombinant pG3.1, pG3.02s, and pG1.m1.02s. Switch plasmids were transfected into LPS-activated B cells, and recombinant plasmids were recovered using the bacterial transformation assay. Switch junctions were identified by automated DNA sequence analysis then by aligning them with germline Sμ (J00440 and J00442), Sγ3 (M12182), and plasmid sequences. Since the germline Sμ sequences J00440 and J00442 overlap by 112 bases, our numbering is based on the combined sequence such that residues 1–5556 are from J00440 and residues 5557–6906 equal 113–1462 of J00442. Sμ.A refers to the Balb/c Sμ sequence, and Sμ.B refers to the partially sequenced Sμ of pG3.1. In pG3.1, the numbering for Sγ3 corresponds to that found for genomic Sγ3 (MUSIGHANA). In pG3.02s and pG1.m1.02s, nucleotide 1 in the plasmid Sγ3 is located at the 5′ end of the Sγ consensus repeat. Brackets around the breakpoints indicate extent of microhomology between the Sμ donor and Sγ3 acceptor sequences, whereas vertical lines at the breakpoint indicate the absence of microhomology. (A) 24 Sμ/Sγ3 recombinant plasmids derived from pG3.1 were analyzed from four independent transfections. (B) 11 Sμ/Sγ3 recombinant plasmids derived from pG3.02s were analyzed from three independent transfections. (C) Eight Sμ/Sγ3 recombinant plasmids derived from pG1.m1.02s were analyzed from two independent transfections. The prefix "Shan" is part of the clone name. (D) Sγ3 recombination breakpoints in the switch plasmids, pG3.02s and pG1.02.m1, were analyzed. A partial schematic diagram of the pG3.02s plasmid is shown at the top. The Sγ3 consensus (hatched) and degenerate (gray) regions are indicated, and the entire DNA sequence of this region is shown at the bottom. The Sγ3 consensus repeat is located at the most 5′ end of the DNA sequence and is underlined. The RGYW and WRCY SHM hotspots are indicated by the horizontal line above the sequence. Switch plasmids were transfected into LPS-activated B cells, and recombinant plasmids were recovered using the bacterial transformation assay. 11 Sμ/Sγ3 recombinant plasmids derived from pG3.02s were analyzed from three independent transfections and are indicated by the arrowheads above the line (M10.LY, T2, Z1, A1, Q62, P22, F143, P15, B36, B12). Eight Sμ/Sγ recombinant plasmids derived from pG1.02.m1 were analyzed from two independent transfections and are indicated by the vertical lines below the sequence (M5, M10, M24, M26, M32, M35, M42, U16).

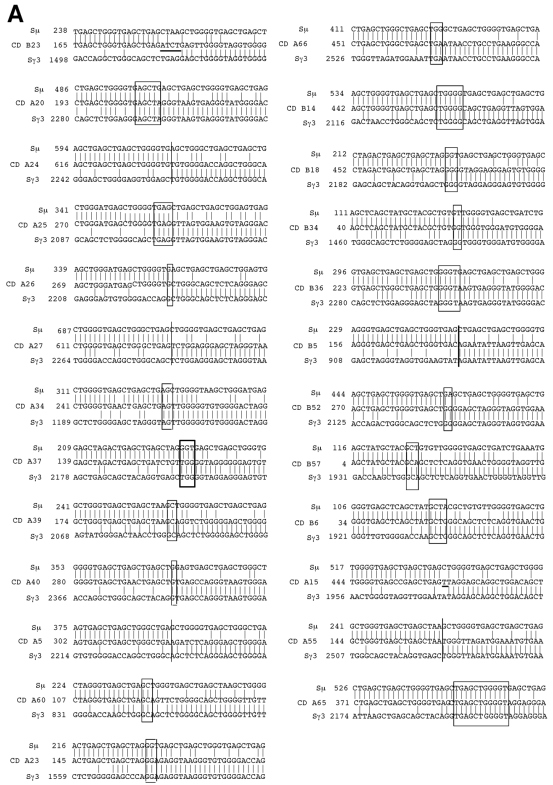

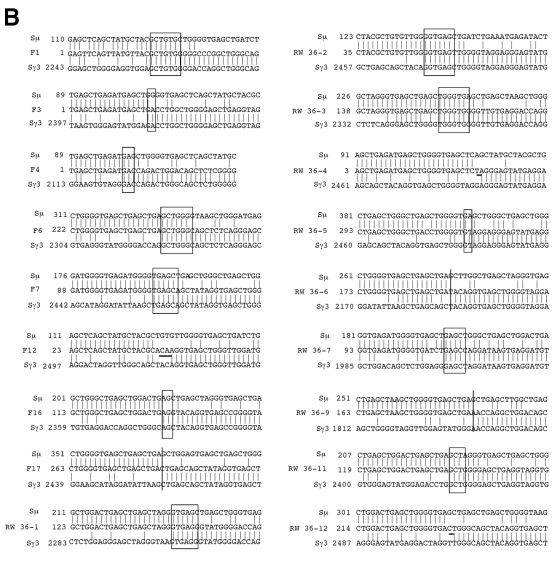

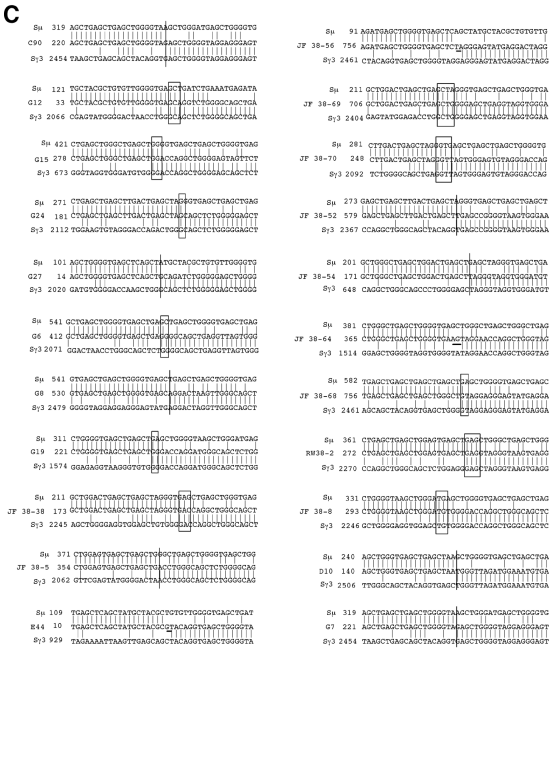

Figure S2. Reduced microhomology is found in Sμ/Sγ3 junctions from p50-deficient mice. Sμ/Sγ3 junctions from $p50^{+/+}$ (A), $p50^{+/-}$ (B), and $p50^{-/-}$ (C) mice were PCR amplified from B cells stimulated with LPS + anti–δ dextran + IL-4 + IL-5 + TGFβ and cloned. At least two independent DNA samples were used as amplification substrates to generate junctions for each group analyzed. Switch junctions were identified by automated DNA sequence analysis and alignment with germline Sμ from the 129 × B6 mice (GenBank/EMBL/DDBJ accession no. AF446347; nt 1 = nt 5206 in MUSIGCD07) and from the sequenced region of Sγ3 from 129 × B6 mice (sequence was a gift from J. Stavnezer). The Sγ3 sequence in E44 best matched the Balb/c Sγ3 sequence (in which nt 1 corresponds to nt 1578 in the GenBank sequence D78343). Underlining indicates sequence, which could not be ascribed to either Sμ or Sγ3. Vertical lines indicate direct abutment of Sμ and Sγ3 DNA, whereas boxed sequence indicates an area of identity and could come from either Sμ or Sγ3. Sequence differences between the parental and recombinant DNAs may be due to mutations introduced during the process of class switch recombination or to PCR errors.

Information for Figure S3. Similar to previous analyses in human cell lines, we found that the MutS components, Msh2 and Msh6 but not Msh3 were substantially more abundant than the MutL constituent Mlh1 (Chang, D.K., L. Ricciardiello, A. Goel, C.L. Chang, and C.R. Boland. 2000. *J. Biol. Chem.* 275:29178). Biochemical evidence demonstrates that Msh2 provides stability to the Msh2/6 and Msh2/3 heterodimers and Mlh1 stabilizes the Mlh1/Pms2 heterodimers (Marra, G., I. Iaccarino, T. Lettieri, G. Roscilli, P. Delmastro, and J. Jiricny. 1998. *Proc. Natl. Acad. Sci. USA.* 95:8568–8573; Drummond, J.T., J. Genschel, E. Wolf, and P. Modrich. 1997. *Proc. Natl. Acad. Sci. USA.* 94:10144–10149). Therefore, our findings predict a stoichiometry of Msh2/6 > Msh2/3 = Mlh1/Pms2 in activated B cells. There was no discernible difference in the level of these transcripts for $p50^{+/+}$ and $p50^{-/-}$ B cells indicating that alteration of mismatch repair (MMR) gene expression is unlikely to have caused the reduction of microhomology at Sμ/Sγ3 junctions derived from p50-deficient B cells. Other MMR proteins, Msh4, Msh5, and Mlh3, are most likely involved in processing of recombination intermediates during meiosis (Nakagawa, T., A. Datta, and R.D. Kolodner. 1999. *Proc. Natl. Acad. Sci. USA.* 96:14186–14188), have not yet been shown to participate in class switch recombination and were not analyzed here.

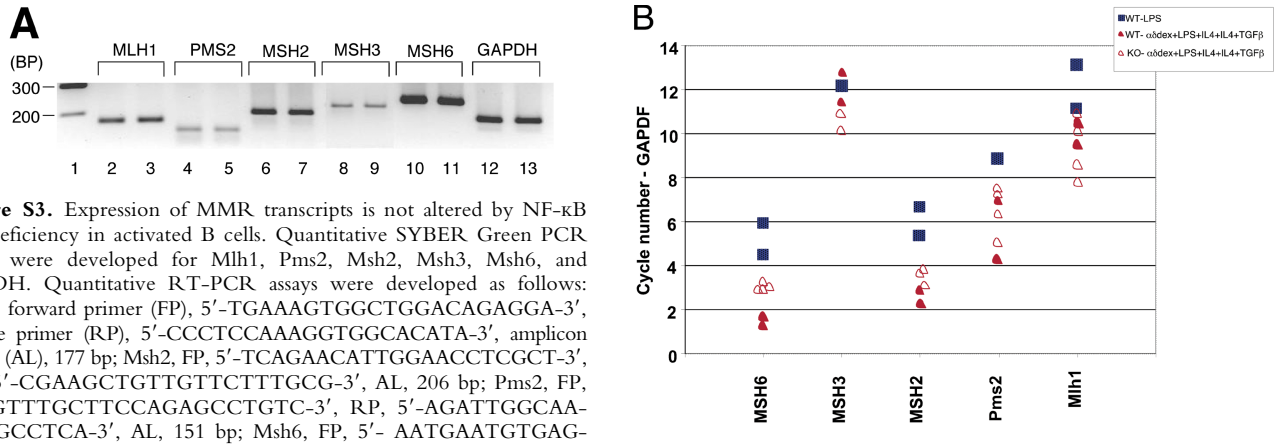

Figure S3. Expression of MMR transcripts is not altered by NF-κB p50 deficiency in activated B cells. Quantitative SYBER Green PCR assays were developed for Mlh1, Pms2, Msh2, Msh3, Msh6, and GAPDH. Quantitative RT-PCR assays were developed as follows: Mlh1, forward primer (FP), 5′-TGAAAGTGGCTGGACAGAGGA-3′, reverse primer (RP), 5′-CCCTCCAAAGGTGGCACATA-3′, amplicon length (AL), 177 bp; Msh2, FP, 5′-TCAGAACATTGGAACCTCGCT-3′, RP, 5′-CGAAGCTGTTGTTCTTTGCG-3′, AL, 206 bp; Pms2, FP, 5′-TGTTTGCTTCCAGAGCCTGTC-3′, RP, 5′-AGATTGGCAACGTGCCTCA-3′, AL, 151 bp; Msh6, FP, 5′- AATGAATGTGAGGACCCCAGC-3′, RP, 5′-AAGGCCAGCAGCCTATGGAT-3′, AL, 251 bp; and Msh3, FP, 5′-TTACCGGATGTCGAGAGAGGA-3′, RP, 5′-AGCTGGCCCATTCAGAACCT-3′, AL, 228 bp. Primers were designed using PrimerExpress (ABI) and used in a real-time assay using SYBR Green PCR Master Mix (ABI) according to the manufactures instructions and an iCycler iQ (Bio-Rad Laboratories). At least two independent RNA samples from each activation state and cell type were reverse transcribed to cDNA and used in the real-time PCR assay. (A) PCR products for the MMR transcripts and GAPDH (lanes 2–13) and a MW standard (lane 1) were visualized by ethidium bromide staining in agarose gels, and molecular weights were verified. Amplified PCR products were DNA sequence verified. (B) Wild-type (solid triangles) and p50-deficient (open triangles) B cells stimulated with LPS + anti–δ dextran + IL-4 + IL-5 + TGFβ and wild-type B cells were also activated with LPS alone (solid squares) for 24 h in two independent cultures, RNA isolated, and cDNA reverse transcribed. Each data point represents an independent cDNA analyzed in duplicate or triplicate and the results averaged. GAPDH is the point of reference, was included in all experiments, and the cycle at which it crossed the threshold was taken as 0. The differences between the threshold cycle for GAPDH and the MMR transcripts are shown.